Supplementary Infromation for

Hybrid graphene/amorphous carbon films with tadpole-like structures for high-performance photovoltaic applications

Tongxiang Cui[1], Ruitao Lv[1*], Zheng-Hong Huang[1], Xin Gan[1], Kunlin Wang[1], Dehai Wu[2], Hongwei Zhu[1,3], Feiyu Kang[1,4*]

[1]*Key Laboratory of Advanced Materials (MOE), School of Materials Science and Engineering, Tsinghua University, Beijing 100084, China*
[2]*Department of Mechanical Engineering and Key Laboratory for Advanced Manufacturing by Materials Processing Technology of Ministry of Education, Tsinghua University, Beijing 100084, China*
[3]*Center for Nano and Micro Mechanics, Tsinghua University, Beijing 100084, China*
[4] *City Key Laboratory of Thermal Management Engineering and Materials, Graduate School at Shenzhen, Tsinghua University, Shenzhen, Guangdong, 518055, China*

* To whom correspondence should be addressed.
E-mails: fykang@tsinghua.edu.cn (F. Kang); lvruitao@tsinghua.edu.cn (R. Lv).

Figures:

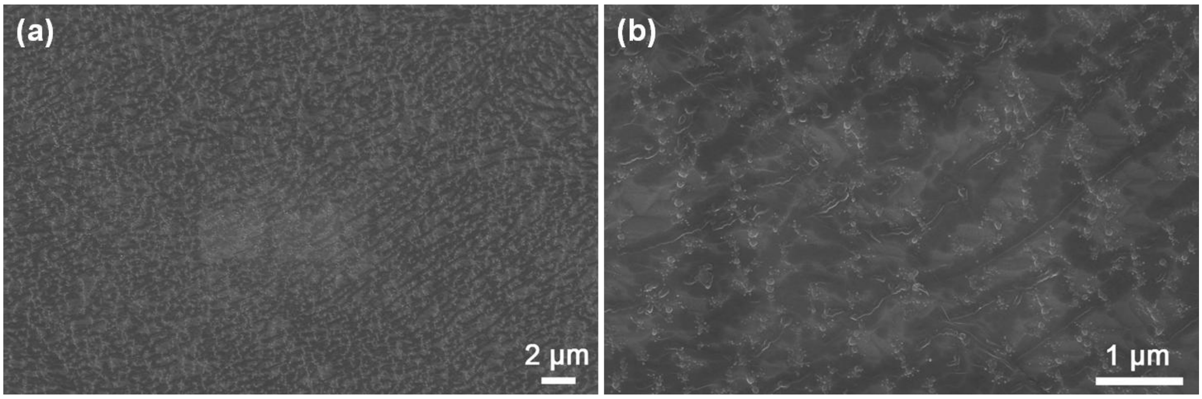

Fig. S1 Typical SEM images of the G/a-C film at different magnifications (a) 10,000 × and (b) 50,000 ×, showing many agglomerates on the surface.

As shown in Figure S2a, the sample contains only carbon without other elements. The peak of Cu in the EDS can be attributed to the TEM grids. The presence of O can be attributed to the exposure of the samples in the air atmosphere.[1] Stainless steel mesh were used to transfer the G/a-C films from $FeCl_3$ solution to deionized water. Minor amount of Fe might come from $FeCl_3$ or stainless steel used during the G/a-C film transferring process. Thus, it is confirmed that agglomerates on the films are mainly composed of carbon. Raman spectra were carried out by randomly selecting six spots in the G/a-C film, as shown in the Figure S2b. All of the spectra consist of three peaks at 1350, 1590, and 2700 cm^{-1} , which correspond to D-band, G-band and 2D-band, respectively. The position of the 2D-band is different at these six spots, which might be attributed to doping, defects or structural difference.[2,3] In addition, the I_{2D}/I_G ratio and the full width at half maximum (FWHM) of 2D-band can be used to distinguish graphene and amorphous carbon.[3,4] One spectrum (green colour) has a I_{2D}/I_G of ~0.6, and a FWHM of ~70 cm^{-1}, showing the Raman spectrum feature of multilayer graphene.[2] One spectrum (blue colour) has a I_{2D}/I_G of ~0.15, and a FWHM of ~80 cm^{-1}, showing the Raman spectrum feature of amorphous carbon.[3]

In order to further investigate the homogeneity of the G/a-C films, Raman mappings were acquired on a 10 μm × 10 μm area of G/a-C film, as shown in Figure S2c. Most of the scrutinized area within the G/a-C film exhibits $I_{2D}/I_G \leq 0.4$, while other area showing $I_{2D}/I_G \geqslant 0.8$. Based on the Raman spectra and Raman mapping of the carbon films, we can see that the films are hybrid multilayer graphene and amorphous carbon.

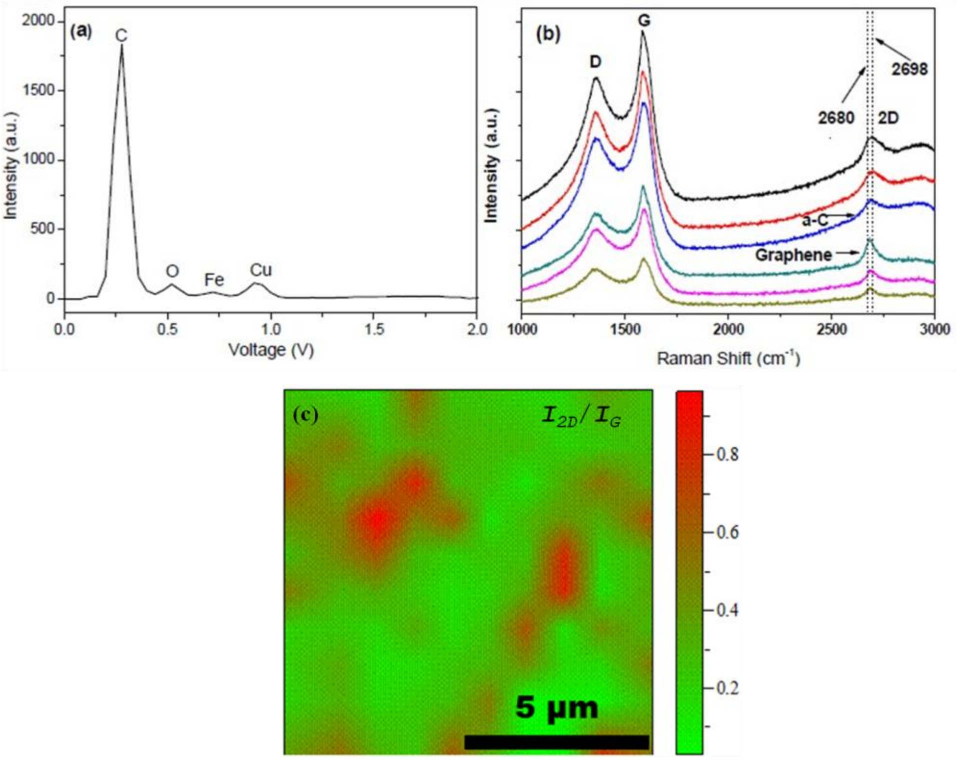

Fig. 2 (a) Typical energy dispersive X-ray spectrum (EDS) of G/a-C films on Cu TEM grid, (b) Raman spectra of as-synthesized G/a-C films on SiO_2/Si wafers, (c) 2D-band to G-band intensity ratio (I_{2D}/I_G) mapping of G/a-C film on SiO_2/Si substrate.

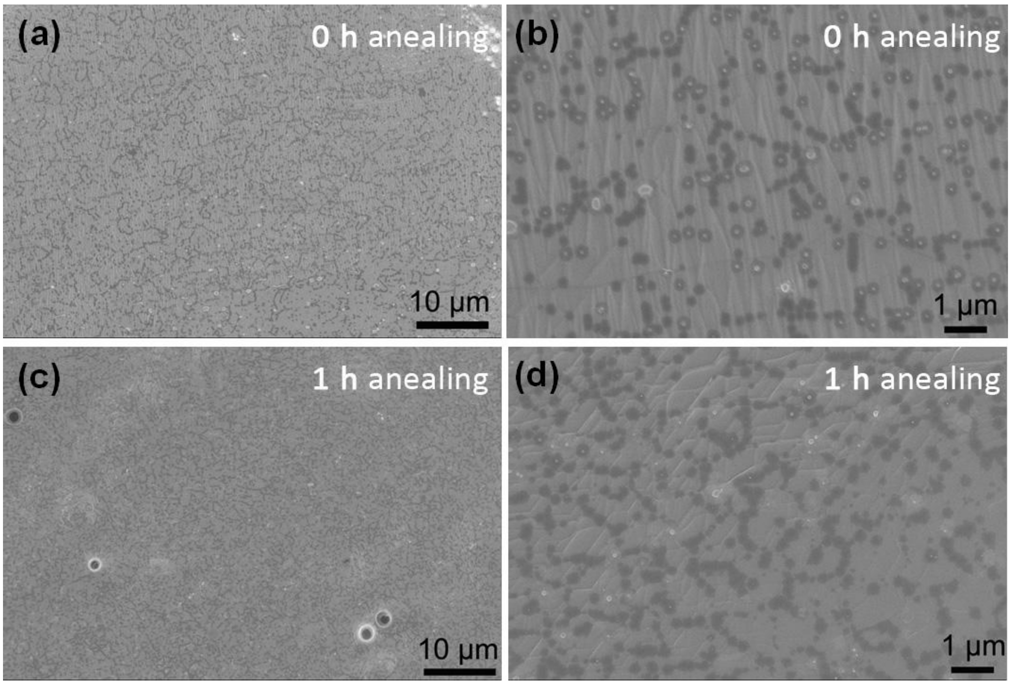

Fig. S3 SEM images of control samples grown on Cu substrates with different annealing times. (a, b) 0 h, (c, d) 1 h.

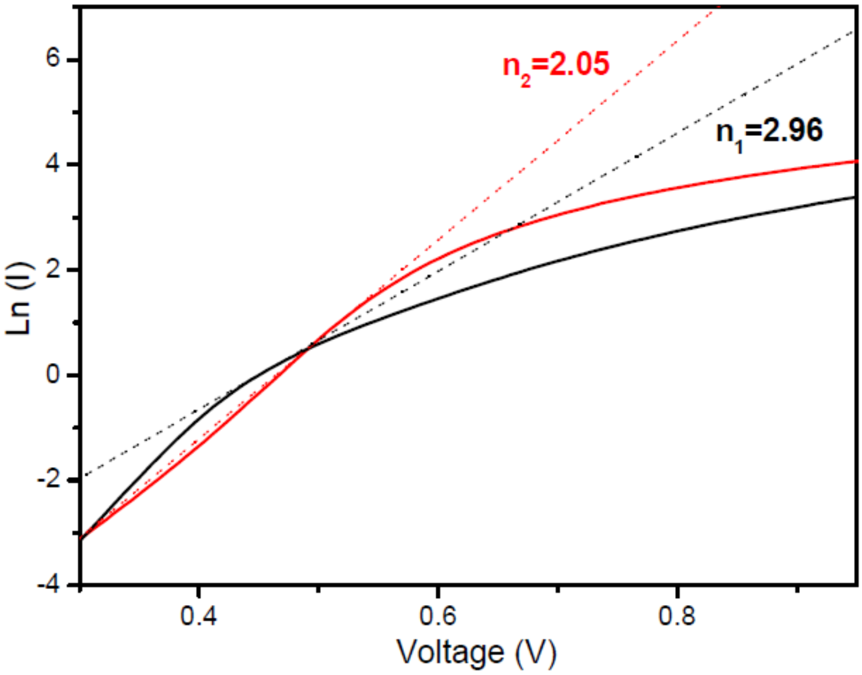

Fig. S4 Napierian logarithm of dark current density (*I*) versus voltage curve, showing the diode ideality factors before (n_1) and after (n_2) HNO_3 treatment, indicating the quality of Si-G/a-C Schottky junction is optimized.

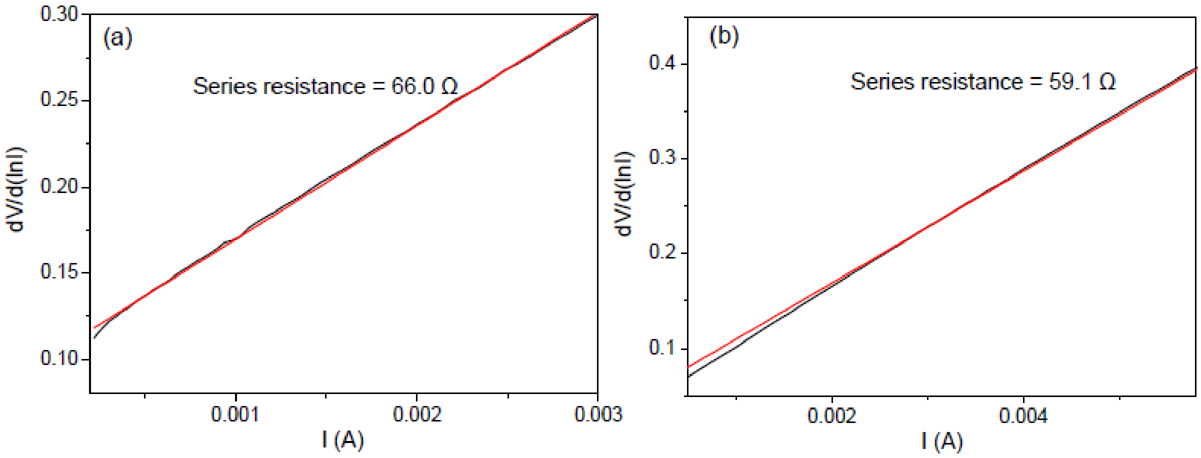

Fig. S5 The series resistance of Si-G/a-C Schottky junction solar cell before and after HNO_3 treatment. (a) before HNO_3 treatment, (b) after HNO_3 treatment. (I is dark current, a liner fit of dV/d(LnI) versus I gives the series resistance of Si-G/a-C Schottky junction solar cell.)

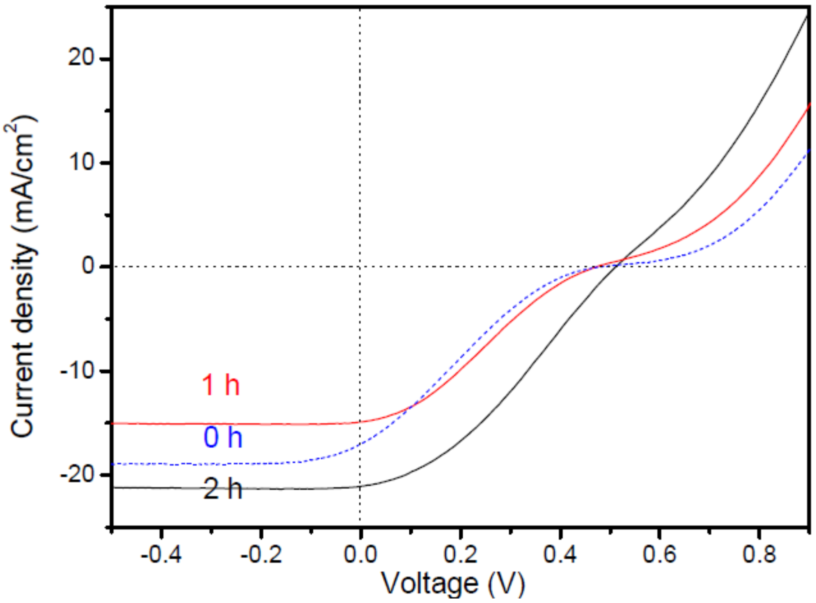

Fig. S6 Light current density-voltage (*J*-*V*) curves of the solar cells based on carbon film produced on Cu substrates with different annealing times.

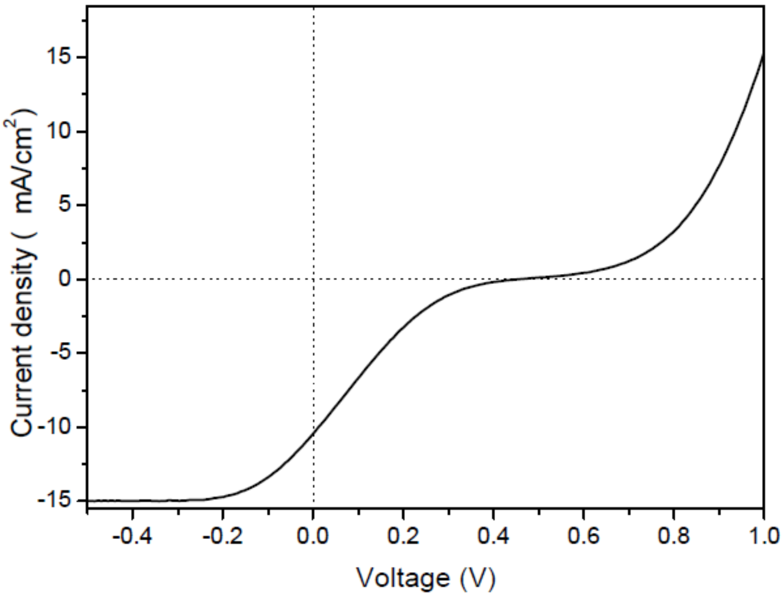

Fig. S7 Light current density-voltage (*J*-*V*) curves of the solar cell based on carbon film produced with an acetonitrile feed rate of 0.08 mL/min.

Tables:

Table S1 The photovoltaic properties of the intrinsic and HNO_3-treated devices.

Conditions	V_{oc}（mV）	J_{sc}（mA/cm^2）	FF	η (%)
Pristine	510.1	21.0	34.1	3.66
HNO_3-1min	547.8	20.5	51.0	5.73
HNO_3-2min	547.8	20.2	52.4	5.78
HNO_3-3min	547.8	20.2	53.2	5.90
HNO_3-4min	555.3	20.0	53.4	5.92
HNO_3-5min	555.3	20.0	53.5	5.95
HNO_3-6min	555.3	20.3	53.5	6.03
HNO_3-7min	555.3	20.4	53.5	6.05
HNO_3-8min	555.3	20.3	53.8	6.07
HNO_3-9min	555.3	20.2	53.6	6.01
HNO_3-10min	555.3	20.3	53.4	6.03
HNO_3-11min	555.3	20.3	54.0	6.07
HNO_3-12min	555.3	20.2	53.5	5.99

Table S2 The photovoltaic properties of the HNO_3-treated devices after being exposed in air for different timescales.

Time after HNO_3 treatment (h)	V_{oc}（mV）	J_{sc}（mA/cm^2）	FF	η (%)
0	555.3	20.3	54.0	6.07
0.5	540.2	20.4	49.9	5.50
1	540.2	20.5	49.5	5.48
4	532.7	21.2	47.2	5.33
12	540.2	21.3	45.8	5.26
24	532.7	20.4	46.6	5.05
48	525.1	20.1	44.4	4.70
96	510.1	20.1	40.9	4.20
192	517.6	18.0	41.3	3.85

References:

1. T. Cui, R. Lv, Z.-H. Huang, F. Kang, K. Wang and D. Wu, ***Nanoscale Res. Lett.***, 2011, 6, 77.
2. A. C. Ferrari, J. C. Meyer, V. Scardaci, C. Casiraghi, M. Lazzeri, F. Mauri, S. Piscanec, D. Jiang, K. S. Novoselov, S. Roth and A. K. Geim, ***Phys. Rev. Lett.***, 2006, 97, 187401
3. Z. H. Ni, Y. Y. Wang, T. Yu and Z. X. Shen, ***Nano Res.***, 2008, 1, 273-291.
4. Z. Li, H. Zhu, D. Xie, K. Wang, A. Cao, J. Wei, X. Li, L. Fan and D. Wu, ***Chem. Commun.***, 2011, 47, 3520-3522.